AIAA JOURNAL
Vol. 37, No. 12, December 1999

Nonlinear Damping Identification from Transient Data

C. B. Smith* and N. M. Wereley†
University of Maryland, College Park, Maryland 20742

To assess the performance of damping augmentation strategies, accurate and reliable nonlinear damping identification techniques are needed. The transient response of a single-degree-of-freedom system having either nonlinear coulomb or quadratic damping is considered. Two analyses for identifying damping from transient test data are evaluated: an analysis based on a periodic Fourier series decomposition and a Hilbert-transform-based technique. Analytical studies for a spectrally isolated mode are used to determine the effects of block length, noise, and error in identified modal frequency on the accuracy of these techniques. The effect of a mode that is spectrally close to the primary mode of interest is also assessed. The primary mode has either coulomb or quadratic damping, and the spectrally close mode is either undamped or has a specified viscous damping level. A comprehensive evaluation of the effects of close mode amplitude, frequency, and damping level is performed. A classifier is also developed to identify the dominant damping mechanism in a signal of unknown composition, based on minimizing the mean square error between the predicted and identified envelope signals.

Nomenclature

$A_1(t_k)$	= Fourier cosine coefficient at time t_k
$a(t)$	= analytical envelope signal
$B_1(t_k)$	= Fourier sine coefficient at time t_k
C_{eq}	= equivalent viscous damping ratio
j	= $\sqrt{-1}$
$x(t)$	= transient signal of interest
$\tilde{y}(t)$	= Hilbert transform of $y(t)$
y_0	= initial (maximum) displacement of transient
ϵ	= quadratic damping ratio
ζ	= viscous damping ratio
μ	= coulomb damping ratio
ϕ	= phase shift of signal
Ω	= frequency of primary mode of interest in transient
ω_n	= natural frequency of transient

Subscripts

c	= coulomb damping quantities
q	= quadratic damping quantities
v	= viscous damping quantities
$\hat{}$	= quantity estimated from experimental data

Introduction

NONLINEAR behavior is present in systems ranging from piping networks[1] to helicopter rotors.[2,3] Elastomeric bearings and electrorheological(ER) or magnetorheological(MR) fluid-filled dampers, which are used in a variety of applications such as exercise equipment and industrial vibration dampers,[4] may also contribute to nonlinear system response. Current studies on MR dampers suggest that a strong coulomb damping characteristic is manifested as the field applied to the MR fluid is maximized. To evaluate the damping performance of these systems, it is necessary to have an accurate and reliable method for identifying nonlinear damping mechanisms.

A particular area of interest at the University of Maryland is damping augmentation in helicopter rotor systems, particularly advanced hingeless or bearingless rotors. With the advent of these new rotor systems, the mechanical complexity of the rotor system is greatly reduced. This reduction is accomplished by replacing the traditional hinges and bearings with a flexure, or flexbeam. This class of rotors is soft in-plane, leading to an increased susceptibility to problems of air and ground resonance. Damping is the major stabilizing influence of both air and ground resonance,[5] and several methods for introducing additional damping into the rotor are being considered.[6–8] Additionally, aeromechanical rotor stability, in which damping is a key factor, has been investigated by several researchers.[9–12] Most recently, Tracy and Chopra[12] looked at the aeromechanical stability of a hingeless rotor with coupled composite flexbeams, whereas Smith and Wereley[6,7] explored the addition of viscoelastic damping layers to composite flexbeams for stability augmentation. Additionally, Kamath et al.[8] investigated the use of MR fluid-filled dampers for increasing the damping level in a bearingless rotor.

The damping in a helicopter rotor may be nonlinear, and although these nonlinear effects may be small, large rotor blade and flexbeam deflections can significantly increase their impact.[13] This paper assesses the accuracy and applicability of two techniques for the identification and estimation of nonlinear damping characteristics from transient data, with special consideration for the applicability to helicopter rotor test data. These techniques are a Fourier-series-based moving block (FSMB) damping analysis and a Hilbert damping analysis based on the Hilbert transform.

Moving block analyses are commonly used in the rotorcraft industry to identify damping of rotor modes such as blade flap, lag, and torsion modes. The helicopter rotor testing environment is especially prone to experimental difficulties in the characterization of damping due to high noise levels and spectrally close modes. Hammond and Doggett[14] used the moving block analysis to perform damping estimates on a rotating scale rotor system in the NASA Langley Research Center transonic dynamics tunnel, whereas Bousman and Winkler[15] described how the moving block analysis could identify damping in spectrally close modes. Use of the moving block analysis to identify rotor stability characteristics was addressed by Tasker and Chopra,[16] who added additional refinements to improve damping estimates, including recursive spectral analysis techniques with improved frequency resolution and windowing to reduce leakage from closely spaced modes. They also assessed this technique for closely spaced modes (both damped and undamped), noisy data, persistent periodic vibrations from undamped modes, and lightly and heavily damped (5%) systems. In 1996, Smith and Wereley[17] applied a similar fast Fourier transform- (FFT-) based moving block analysis to analytical signals with linear viscous damping that included noisy data, spectrally close modes, and errors in the excitation frequency. This technique was then used to identify the linear viscous damping level in experimental transients obtained from both stationary and

Presented as Paper 98-2003 at the AIAA/ASME/ASCE/AHS/ASC 39th Structures, Structural Dynamics, and Materials Conference, Long Beach, CA, 20–23 April 1998; received 31 August 1998; revision received 3 May 1999; accepted for publication 5 May 1999.

*Graduate Research Assistant, Alfred Gessow Rotorcraft Center, Department of Aerospace Engineering; splash@eng.umd.edu.

†Associate Professor, Alfred Gessow Rotorcraft Center, Department of Aerospace Engineering, 3181 Engineering Classroom Building; wereley@eng.umd.edu.

rotating composite beams with viscoelastic damping layers. However, when the FFT-based moving block technique was extended to nonlinear damping, the damping level estimates were found to be extremely sensitive to the length of the data block used in the analysis, having as much as 100% error in the identified equivalent viscous damping.[18] The primary difficulty is that very short block lengths, which lead to poor frequency resolution, produce the most accurate damping level estimates. However, in a spectrally dense environment (such as a helicopter rotor), a necessary feature of the damping analysis must be excellent frequency resolution to differentiate between spectrally close modes. Because it is not possible to obtain both excellent frequency resolution and accurate damping level estimates at the same time, the FFT-based moving block analysis is not suitable for nonlinear damping identification.

A moving block damping identification technique based on a periodic Fourier series decomposition was developed to mitigate the problems associated with the FFT-based moving block analysis. In this method, the periodic Fourier series decomposition is performed at the frequency of interest to spectrally isolate the mode of interest. Because of this spectral isolation, a block length duration of only a single period of data will accurately identify the damping level in a transient response without the associated loss in frequency resolution.

Finally, a damping identification technique based on the Hilbert transform[19] is considered. The determination of damping from a transient response, whether linear or nonlinear, can be reduced to determination of the decay envelope. The Hilbert transform is the standard transform used in envelope detectors and is uniquely capable of computing the transient decay envelope. Agneni and Crema[20] first suggested this technique for time-domain damping identification, whereas Smith and Wereley[6] used a Hilbert-transform-based technique to identify the linear viscous damping level in both stationary and rotating composite beams with viscoelastic damping layers using time-domain transient data. Further, an assessment was made of the effects of noisy data, spectrally close modes, and error in excitation frequency.[6] Simon and Tomlinson[21] used the Hilbert transform to identify the presence of nonlinear damping effects using frequency-domain data, but neither the damping mechanism nor the damping level was identified.

The objective of this paper is to classify nonlinear damping in a transient response based on the shape of the envelope signal, as well as to quantify the nonlinear damping level. To accomplish this, two nonlinear damping identification techniques are developed and validated using synthetic transients with known coulomb and quadratic damping levels. Both isolated modes and spectrally dense environments will be considered. For an isolated mode, the effects of block length, noise, and error in excitation frequency will be considered. In the case of a spectrally close mode, the effects of the amplitude, frequency, and damping level of the close mode will be evaluated. A classification technique for determination of the dominant damping mechanism in a transient will also be presented.

Nonlinear Damping Mechanisms

To evaluate the performance of the Hilbert and FSMB damping analyses when used to identify nonlinear damping, it is necessary to know the type and level of damping in the system. To accomplish this, transients for single-degree-of-freedom (SDOF) systems with both coulomb and quadratic damping were generated via an initial condition response to a nonzero initial displacement using an ordinary differential equation solver in MATLAB®. Table 1 includes the governing equations, envelope signal expressions, and equivalent viscous damping expressions for coulomb, viscous, and quadratic damping. Viscous damping is shown for comparison.

Coulomb Damping

Coulomb damping is associated with surface or rubbing friction, also known as dry friction. The equation of motion for an SDOF system with coulomb damping is given by

$$\ddot{x} + \mu(\dot{x}/|\dot{x}|) + \omega_n^2 x = 0 \tag{1}$$

where μ is the coulomb damping ratio and ω_n is the natural frequency. The envelope of the response is given analytically by

$$a_c(t) = -(2\mu/\pi\omega_n)t + y_0 \tag{2}$$

Once the envelope signal $\hat{a}(t)$ has been determined from the transient test data, estimates for the coulomb damping ratio μ and the equivalent viscous damping $C_{\text{eq},c}$ can be determined.

To estimate the coulomb damping ratio μ, a cost function $J_c(t)$ was defined as the least mean square (LMS) error between the analytical and estimated envelope signals. The cost function was minimized over μ, resulting in an estimate for the coulomb damping ratio $\hat{\mu}$ as

$$\hat{\mu} = \min J_c(\mu) = \min \sum_{i=1}^{N} [a_c(t_i) - \hat{a}(t_i)]^2 \tag{3}$$

The equivalent viscous damping $C_{\text{eq},c}$, can be calculated in one of two ways. If the coulomb damping ratio estimate $\hat{\mu}$ is available, $C_{\text{eq},c}$ may be found analytically as follows:

$$C_{\text{eq},c}(t) = \frac{2\hat{\mu}}{\pi\omega_n^2 a_0 - 2\hat{\mu}\omega_n t} \tag{4}$$

where a_0 is the initial amplitude of the transient/envelope signal. Otherwise, the slope between any two points of the log of the envelope signal can be defined as $-\zeta\omega_n$, and given the natural frequency, the equivalent viscous damping ratio may be determined. Three different coulomb damping ratios, $\mu = 100, 300$, and 500, were used in this study to simulate light, moderate, and heavy damping, respectively. An example of a transient with coulomb damping ($\mu = 300$) and 5% noise is shown in Fig. 1a. The addition of 5% noise corresponds to the addition of a normally distributed signal having zero mean and a variance of 5% of the initial amplitude of the transient being studied.

Quadratic Damping

Air damping can be represented as quadratic damping, as in the air resistance of a moving structure. The governing equation of an SDOF system with quadratic damping is

$$\ddot{x} + \epsilon|\dot{x}|\dot{x} + \omega_n^2 x = 0 \tag{5}$$

where the response of this system is

$$y(t) = a_q(t)\sin[\omega_n(t) + \beta(t)] \tag{6}$$

Here the envelope signal is

$$a_q(t) = \frac{3\pi a_0}{3\pi + 4\epsilon\omega_n a_0 t} \tag{7}$$

Once the envelope signal $\hat{a}(t)$ has been estimated from transient test data, estimates for ϵ and $C_{\text{eq},q}$ can be determined.

Table 1 Coulomb, viscous, and quadratic damping mechanisms

Damping type	Governing equation (homogeneous form)	Envelope signal	Equivalent viscous damping coefficient
Coulomb	$\ddot{x} + \mu\dfrac{\dot{x}}{\lvert\dot{x}\rvert} + \omega_n^2 x = 0$	$a_c(t) = \dfrac{-2\mu}{\pi\omega_n}t + y_0$	$C_{\text{eq},c}(t) = \dfrac{2\hat{\mu}}{\pi\omega_n^2 a_0 - 2\hat{\mu}\omega_n t}$
Viscous	$\ddot{x} + 2\zeta\omega_n\dot{x} + \omega_n^2 x = 0$	$a_v(t) = e^{-\zeta\omega_n t}$	$C = 2\zeta\omega_n$
Quadratic	$\ddot{x} + \epsilon\lvert\dot{x}\rvert\dot{x} + \omega_n^2 x = 0$	$a_q(t) = \dfrac{3\pi a_0}{3\pi + 4\epsilon\omega_n a_0 t}$	$C_{\text{eq},q}(t) = \dfrac{4\hat{\epsilon}a_0}{3\pi + 4\hat{\epsilon}\omega_n a_0 t}$

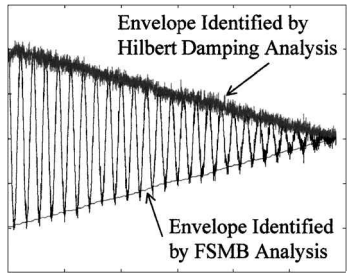

a) Coulomb damping, 5% noise

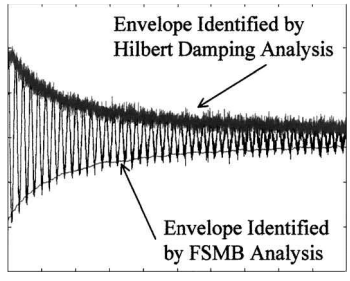

b) Quadratic damping, 5% noise

Fig. 1 Examples of identified envelope signals from Hilbert and FSMB damping analyses.

To estimate the quadratic damping ratio ϵ, a cost function $J_q(t)$ was defined as the LMS error between the analytical and estimated envelope signals. The cost function was minimized over ϵ, resulting in an estimate for the quadratic damping ratio $\hat{\epsilon}$:

$$\hat{\epsilon} = \min J_q(\epsilon) = \min \sum_{i=1}^{N} [a_q(t_i) - \hat{a}(t_i)]^2 \tag{8}$$

As in the coulomb damping case, the equivalent viscous damping coefficient can be calculated in one of two ways. If $\hat{\epsilon}$ is available, $C_{\text{eq},q}$ may be determined analytically:

$$C_{\text{eq},q}(t) = \frac{4\hat{\epsilon} a_0}{3\pi + 4\hat{\epsilon}\omega_n a_0 t} \tag{9}$$

where a_0 is the initial amplitude of the transient/envelope signal. If $\hat{\epsilon}$ is not available, the slope between any two points of the log of the envelope signal can be defined as $-\zeta\omega_n$, and $C_{\text{eq},q}$ at that time may be easily determined. Three quadratic damping ratios are considered, $\epsilon = 0.003$, 0.005, and 0.007, to simulate systems with light, moderate, and heavy quadratic damping. An example of a transient with quadratic damping ($\epsilon = 0.005$) and 5% noise is shown in Fig. 1b.

Damping Identification Techniques

To identify coulomb and quadratic damping levels, the critical step is the identification of the envelope signal $\hat{a}(t)$. The damping mechanism can be classified by the shape of the envelope signal (for example, linear decay for coulomb damping). The decay rate of the envelope signal and the natural frequency are then used to determine the damping level. Two methods to estimate the envelope signal are presented: 1) a moving block analysis based on the Fourier series decomposition at the frequency of interest and 2) a Hilbert-transform-based analysis. For each method, it is assumed that a transient decay response is available based on either an impulse response (to identify damping of the primary mode) or a steady-state sinusoidal excitation/response pair at the modal frequency of interest, where the sinusoidal excitation is terminated at peak amplitude and the ensuing transient response acquired. The peak amplitude of each transient is also determined, and when the amplitude of the transient drops below a specified value, the data set is truncated for analysis. This specified value is the threshold cutoff value and has a significant effect on the identified damping level. The purpose of the threshold cutoff value is to minimize the effects of noise and persistent excitation on the results of the damping identification analysis.

Modal Frequency Identification

A key element of damping identification is accurate knowledge of the modal frequency of interest. The first, and preferable, method for modal frequency identification is a standard steady-state frequency response function measurement, ensuring high-frequency resolution. For example, using a sine sweep focused around the mode of interest, it is routine to achieve frequency resolutions of $\Delta f = 0.1$–0.01 Hz using excitation signal durations of from $T = 10$ s to $T = 100$ s. The second, and more problematic, approach is to take the FFT of the measured transient. In this case, the frequency resolution is equal to the inverse of the time span of the original transient. Frequency resolution for a spectrally isolated mode can be improved by padding zeros onto the end of the transient to increase the duration of the signal and, thereby, increase the frequency resolution of the FFT.

Once the modal frequency of interest, Ω, has been identified, the envelope signal can be identified from the transient data. Two techniques for accomplishing this are the FSMB damping analysis and the Hilbert damping analysis.

FSMB

To avoid some of the limitations of the FFT-based moving block discussed earlier, a different moving block analysis was developed. Tasker and Chopra[16] used Hamming's local Fourier series solution, which is a recursive technique used to calculate the Fourier coefficients for slowly time-varying signals. This algorithm depends greatly on the concept of a slowly changing envelope signal. In cases where the damping level is high (>1%), the envelope signal may not be slowly changing, and Hamming's solution may not be the most appropriate choice. Here, a simple compromise is made, sacrificing some computational speed to accurately identify envelope signals for transients associated with equivalent viscous damping levels greater than 1%. In this case, a nonrecursive periodic FSMB analysis is used. It maintains the frequency resolution advantage of Goertzel's algorithm as described by Tasker and Chopra,[16] while sacrificing slightly the speed gained by recursion. In return, this technique does not require that the signal be slowly time varying and can, therefore, more accurately identify higher damping ratios.

In this method, the signal is assumed to be of the form

$$x(t) = A_1 \cos(\Omega t) + B_1 \sin(\Omega t) \tag{10}$$

where the Fourier coefficients are

$$A_1(t_k) = \int_{t_k}^{t_k + (2\pi N_c/\Omega)} x(t) \cos(\Omega t)\, \mathrm{d}t \tag{11}$$

$$B_1(t_k) = \int_{t_k}^{t_k + (2\pi N_c/\Omega)} x(t) \sin(\Omega t)\, \mathrm{d}t \tag{12}$$

with N_c the block length in number of cycles of data, where each cycle corresponds to a period of duration $2\pi/\Omega$ and t_k the time of the kth sample in the transient. These coefficients are calculated for the data window at time t_k, and then the window of data is moved forward one data point and the coefficients are recalculated. Thus, $A_1(t_k)$ and $B_1(t_k)$ are the average in phase and quadrature amplitudes of $x(t)$ at time t_k. This process is repeated for the number of iterations desired, $k = 1, 2, 3, \ldots, N_{\text{iter}}$, and the envelope is then estimated using the following relation:

$$\hat{a}(t_k) = \sqrt{A_1(t_k)^2 + B_1(t_k)^2} \tag{13}$$

Once the envelope has been determined, the damping level may be identified for the particular damping mechanism under consideration.

An online damping estimate would be desirable, particularly in situations such as rotor testing. Unlike the FFT-based moving block algorithm, this Fourier-series-based technique is much less computationally intensive. As a result, this method lends itself to online implementation in the same way as Goertzel's algorithm.[16]

Hilbert Damping Analysis

Damping estimation reduces to the determination of the amplitude of the decay envelope signal from a transient structural response. The amplitude of the envelope signal between peak points of the dispersive transient response is intuitive; however, as stated earlier, most damping estimation techniques do not directly address determination of the envelope signal. In contrast, the Hilbert transform of a real valued signal, $y(t)$, provides a means for calculating this envelope signal directly.[19]

The Hilbert transform is a linear integral transform. However, a more useful definition of the Hilbert transform is as a 90-deg phase shift system. The Hilbert transform can be thought of as passing a signal through a filter that leaves its magnitude unchanged, but shifts the phase by 90 deg for positive frequencies. Thus, $\tilde{y}(t)$ is simply $y(t)$ shifted by 90 deg. Thus, for the case of quadratic damping, the decaying transient is given by

$$y(t) = a_q(t)\cos(\omega_n t + \phi) \tag{14}$$

The Hilbert transform is then the signal, phase shifted by 90 deg, as

$$\tilde{y}(t) = a_q(t)\sin(\omega_n t + \phi) \tag{15}$$

We define an analytic signal

$$z(t) = y(t) + j\tilde{y}(t) \tag{16}$$

as the sum of the real signal $y(t)$ plus an imaginary Hilbert transform signal $j\tilde{y}(t)$. The phasor form is

$$z(t) = a_q(t)e^{j\theta(t)} \tag{17}$$

where $a_q(t)$ is the envelope signal of $y(t)$ and $\theta(t)$ is the instantaneous phase signal of $y(t)$. The envelope signal is given by

$$a_q(t) = \sqrt{y(t)^2 + \tilde{y}(t)^2} \tag{18}$$

Once the envelope signal has been determined, the damping level may be identified for the particular damping mechanism under consideration.

As in the FSMB analysis, the Hilbert damping analysis is much less computationally intensive than the FFT-based moving block technique. Therefore, the Hilbert damping analysis is also a good candidate for online implementation.

Typical Envelope Signals

Accurate identification of the envelope signal from transient data is critical to both damping identification techniques considered here. Figure 1 shows the difference between envelope signals identified by the Hilbert damping analysis and those identified by the FSMB damping analysis. It is easily seen that the upper envelope signal, identified using the Hilbert damping analysis, contains more high-frequency information than the lower envelope, identified using the FSMB damping analysis. This high-frequency content comes from the 5% noise present in the transient signals shown. The FSMB analysis exhibits a smoothing or averaging effect on the envelope, providing a smoothed envelope for analysis. A similar effect could be obtained by low-pass filtering the envelope signal obtained using the Hilbert damping analysis.

Damping Identification for Isolated Modes

To evaluate the performance and effectiveness of both damping identification techniques, nonlinear coulomb and nonlinear quadratic damping mechanisms are investigated via simple simulation studies. The effects on damping estimates by changes in block length and noise level are investigated. To better understand the effects of these factors on the accuracy of the damping identification algorithms used in this study, a single spectrally isolated mode was chosen for analysis. In this case, a natural frequency of 9 Hz was chosen, as it is nominally the first lag frequency of the Froude-scaled bearingless composite rotor in our experimental setup at the University of Maryland. Typically, the frequency of interest may not be previously known; however, it has been shown that if the frequency of interest can be identified within approximately 0.5 Hz, reasonable results may be obtained.[22] As described earlier, this frequency

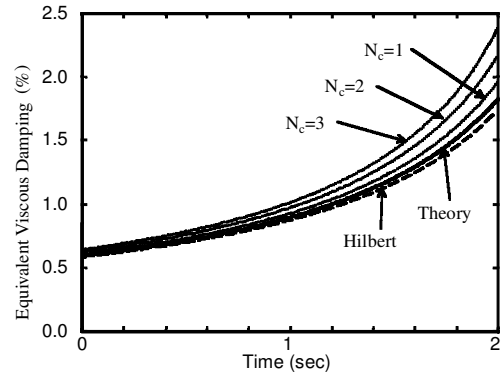

a) Equivalent viscous damping vs time

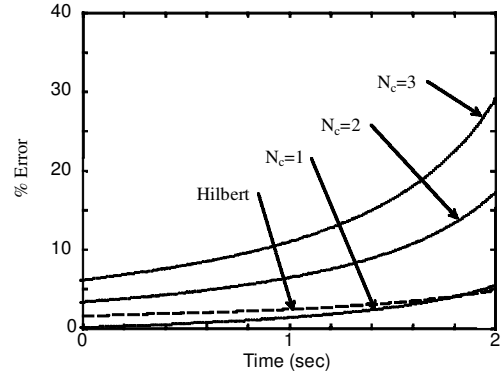

b) % Error vs time

Fig. 2 FSMB damping analysis of a signal with coulomb damping and 10% noise, effects of block length.

identification is possible by performing an FFT of the data set under consideration. If the transient data set is at least 2 s in duration, the frequency resolution will be at least 0.5 Hz, which is adequate to identify the damping ratio with reasonable accuracy. If the transient is shorter than 2 s, zeros may be padded onto the end of the data set to reach the required length.

Effects of Block Length

An important parameter in any moving block analysis is the choice of the data block length. In the FSMB damping analysis, this is measured in the number of cycles (or periods), N_c, used. The results of varying the number of cycles used in the FSMB damping analysis with 10% noise are shown in Figs. 2 and 3. It is evident that, as the number of cycles is decreased, that is, as fewer data points are used in each computation, the equivalent viscous damping estimate improves. Unlike the FFT-based technique, however, there is no loss of frequency resolution because the Fourier coefficients are calculated at a specific predetermined frequency Ω. Thus, there is no penalty for reducing the number of cycles in the moving block, and this technique can accurately be used to identify nonlinear damping mechanisms such as coulomb and quadratic damping. Therefore, for all further analyses, the FFT-based moving block will be dropped from consideration, and only the Fourier-series-based moving block and the Hilbert damping analyses will be considered.

Effects of Noise

Another concern when trying to identify the damping level in an experimental data set is the presence of noise. To identify the effects of noise on the accuracy of the damping identification analyses, analytical transients with varying noise levels (0, 1, 5, and 10%) were generated. As described earlier, the addition of 5% noise corresponds to the addition of a signal with a normal distribution of random values with a mean of zero and a variance of 5% of the initial amplitude of the transient being studied. These transients were analyzed using both the Hilbert and FSMB analyses. Equivalent viscous damping estimates for the coulomb and quadratic damping

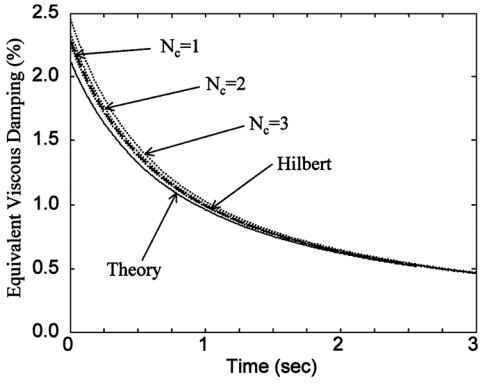

a) Equivalent viscous damping vs time

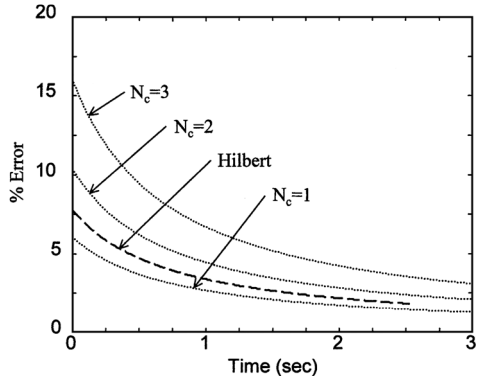

b) % Error vs time

Fig. 3 FSMB damping analysis of a signal with quadratic damping and 10% noise: effects of block length.

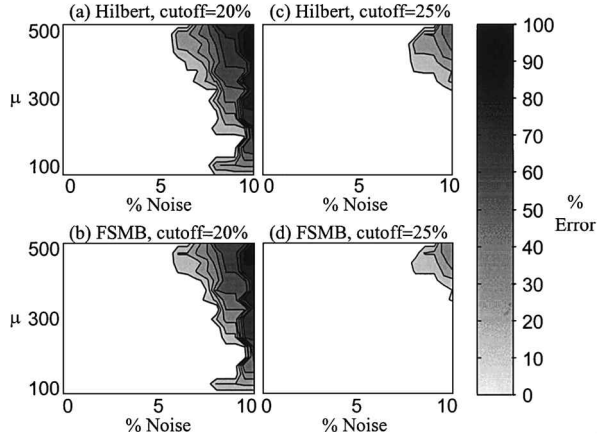

Fig. 4 Effects of varied noise level on the identified damping in an isolated mode with varied coulomb damping ratio.

mechanisms with 10% noise are shown in Figs. 2 and 3, respectively. Analytical results are also shown for comparison. It can be seen from Fig. 2 that, for coulomb damping with 10% noise, the Hilbert damping analysis outperforms the FSMB damping analysis. In the case of quadratic damping with 10% noise, however, Fig. 3 shows that the FSMB damping analysis performs slightly better than the Hilbert damping analysis.

To better understand the effects of noise on the identified damping level, a series of transients was generated in which the coulomb damping ratio μ was varied over a range of 100–500 in increments of 25, and the quadratic damping ratio ϵ was varied over a range of 0.003–0.007 in increments of 0.00025. In addition, the noise level was varied from 0 to 10% in increments of 0.5%. These transients were analyzed using both damping identification techniques, and the percent error between actual and identified damping levels was calculated. This matrix of error values was then used to generate the contours of constant error shown in Figs. 4 and 5.

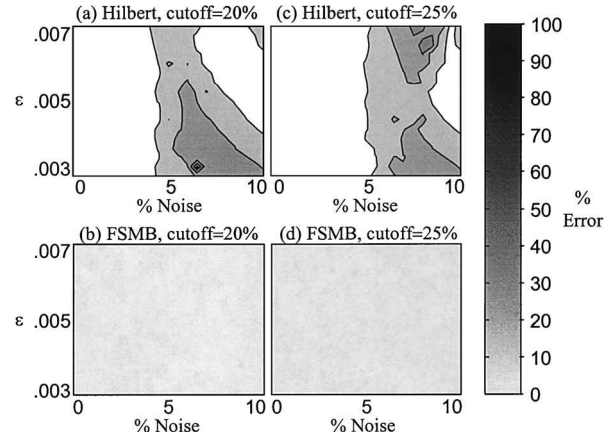

Fig. 5 Effects of varied noise level on the identified damping in an isolated mode with varied quadratic damping ratio.

It can be seen in Fig. 4 that for a single mode with coulomb damping, low noise levels <5% have very little or no effect on the identified damping level. As the noise level increases beyond 5%, the error in the identified damping level may begin to increase as well. It may also be seen that there is a strong dependence on the threshold cutoff value used in the analysis. As the threshold value is raised, the error for a given noise level is reduced. As an example, for 8% noise and a threshold cutoff of 20%, the error can be as large as 50%. At this same noise level, a threshold cutoff of 25% will result in an error no higher than 15%. It can also be seen from Fig. 4 that both the Hilbert damping analysis and the FSMB damping analysis produce qualitatively similar results.

Figure 5 shows the effects of noise on a single mode with quadratic damping. In the case of the Hilbert damping analysis, the lower threshold cutoff values provide slightly better performance than the higher values, indicating the importance of careful threshold selection. If the threshold is set too low, noise and persistent excitation can corrupt the identified envelope, whereas if the threshold is set too high, not enough signal remains to accurately identify the geometry of the envelope and its corresponding damping ratio. This problem is not as serious in the coulomb case, where the envelope is linear and is easily defined. The results for the FSMB show very little variation in error over the entire range of noise and damping levels. This is attributed to the averaging effect of the FSMB mentioned earlier.

In general, it should be noted that the threshold cutoff value should be set higher than any background noise or persistent excitation whenever possible. Further, the shape of the envelope signal is a critical factor in accurate damping identification. Defining this shape accurately is, therefore, one of the most important considerations when determining the most effective cutoff level.

Damping Identification for Spectrally Close Modes

To more closely emulate helicopter rotor system test data, these techniques were then applied to a signal composed of two closely spaced modes. These data were developed to simulate a response containing the first lag and 1/revolution modes. The primary mode of interest (simulated lag mode) had either coulomb or quadratic damping, and the close mode (1/revolution) was either undamped or had a specified amount of viscous damping. A comprehensive evaluation of the effects of close mode amplitude, frequency, and damping level was then performed. In these studies, the coulomb damping ratio μ was varied over a range of 100–500 in increments of 25, and the quadratic damping ratio ϵ was varied over a range of 0.003–0.007 in increments of 0.00025.

Assessing the Close Mode

When determining the effectiveness of the techniques considered here in identifying damping in the presence of a spectrally close mode, several parameters need to be considered. The first parameters that need to be identified are the frequencies of both the primary mode f_p and the spectrally close mode f_c. The difference between these frequencies, Δf, is an important quantity in determining the

effectiveness of the damping analyses. Another important parameter is the amplitude ratio of the close mode to the primary mode. As the amplitude ratio grows larger, the spectrally close mode has a more significant effect on the shape of the transient, and the error in the identified damping level will grow larger as well. As already discussed, the preferred method for identification of these parameters is a standard steady-state frequency response function measurement, ensuring high-frequency resolution. If these data are not available, it may be possible to use an FFT of the transient response to identify these parameters, although noise and persistent excitation can make it difficult to isolate the frequencies and amplitudes of the spectrally close modes. These difficulties can arise from poor frequency resolution and/or a high-amplitude ratio between the close and primary modes, especially if the damping in the close mode is less than the damping in the primary mode. Again, it is important to have good frequency resolution to accurately identify these parameters and to determine the effectiveness of the damping analysis being considered.

Effects of Close Mode Amplitude

One concern in the identification of damping in a spectrally dense environment is the amplitude of the modes that surround the mode of interest. To determine the effect of the amplitude of a close mode, an analytical signal was created that consisted of a primary mode of interest at 9 Hz and a close, undamped mode of varying amplitude at 10 Hz. This results in a Δf of 1 Hz between the two modes. The ratio of the amplitude of the close mode to the amplitude of the primary mode was varied from 0.0 to 1.0 in increments of 0.05, and these transients were analyzed using both the Hilbert and FSMB damping identification techniques. The percent error between actual and identified damping level was calculated, and this matrix of error values was then used to generate the contour plots shown in Fig. 6 for coulomb damping and Fig. 7 for quadratic damping.

It can be seen from Fig. 6 that, for a primary mode with coulomb damping, if the amplitude of the close mode is lower than the cutoff threshold set in the analysis (in this case, 30%), the impact of the persistent excitation on the damping analysis is negligible. On the other hand, if the amplitude of the close mode is higher than the cutoff, the persistent excitation has a significant impact on the damping estimate, and the error grows rapidly from 30% or less to near 100%.

For the case of a primary mode with quadratic damping, the contour plots shown in Fig. 7 exhibit a different phenomenon. For a Δf of 1 Hz, a slightly more complicated pattern than that seen in the coulomb damping case emerges. The error remains relatively low until the threshold (again 30%) is reached, with one exception. Areas of higher error are present at an amplitude ratio of between 0.2 and 0.3, resulting in the contours seen in Fig. 7. Although the close mode amplitude is less than the cutoff value, the sum of the close mode and the primary mode together can be greater that this threshold, increasing the error in the identified damping level. As with random noise, the threshold cutoff value should be set higher than the amplitude of the close mode by a reasonable amount (>5–10%) whenever possible to avoid this problem, but as discussed earlier, care must be taken to preserve enough of the signal for accurate identification of the envelope geometry and damping ratio.

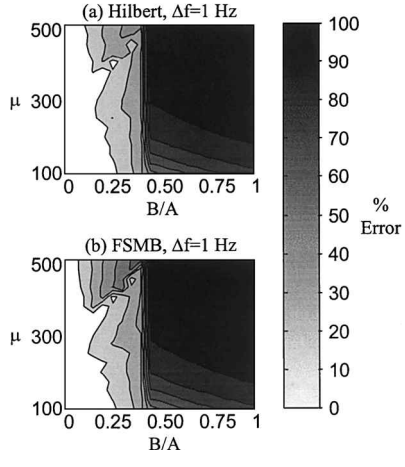

Fig. 6 Effects of the varied amplitude ratio of a spectrally close, undamped mode on the identified damping level in a primary mode with varied coulomb damping.

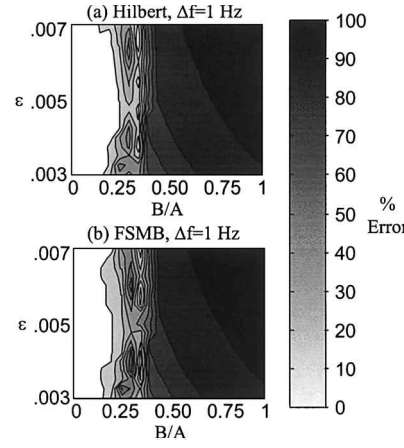

Fig. 7 Effects of the varied amplitude ratio of a spectrally close, undamped mode on the identified damping level in a primary mode with varied quadratic damping.

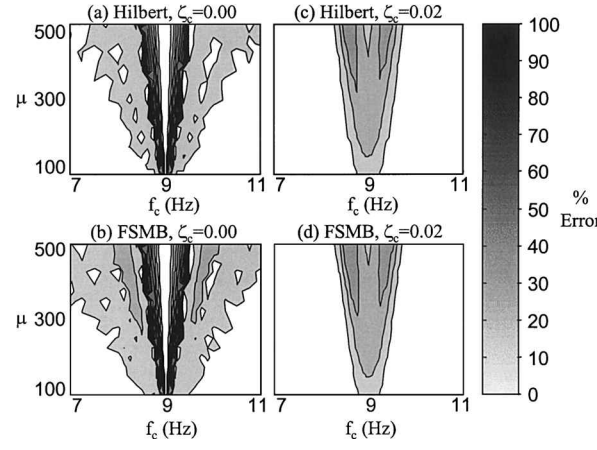

Fig. 8 Effects of a spectrally close mode with varied frequency on the identified damping in a primary mode with varied coulomb damping ratio.

Effects of Close Mode Frequency

Another concern in the identification of damping in a spectrally dense environment is the frequency separation of the modes. To study this phenomenon, an analytical signal was created that consisted of a primary mode of interest at 9 Hz and a close mode with a viscous damping ratio of either 0.00 or 0.02. The frequency of this close mode was varied from 7 to 11 Hz in varying increments, with the smallest increments being concentrated around 9 Hz. The transients were analyzed using both damping identification techniques, and the percent error between actual and identified damping level was calculated as before. Contour plots of constant error generated by both the Hilbert analysis and the FSMB analysis are shown for coulomb damping in Fig. 8 and for quadratic damping in Fig. 9. It can be seen from the coulomb results shown in Fig. 8 that if the close mode is undamped and is at the same frequency as the primary mode both damping identification techniques perform very well. However, if the frequency of the close mode is shifted slightly (<1 Hz), the error grows quickly. If the frequency is then shifted even farther away from the frequency of the primary mode (≥1 Hz), the error begins to decrease again. For a close mode with viscous damping of 2%, shown in Figs. 8c and 8d, similar trends are observed; however, the error with matching frequencies is slightly higher, whereas the error when the frequency separation is small is lower than in the undamped close mode case. Similar behavior is observed in the quadratic damping results shown in Fig. 9.

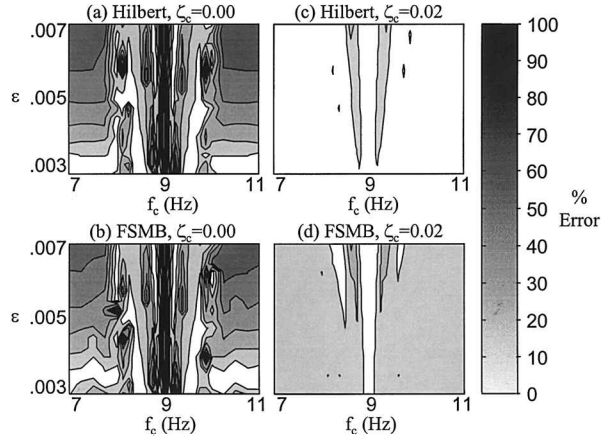

Fig. 9 Effects of a spectrally close mode with varied frequency on the identified damping in a primary mode with varied quadratic damping ratio.

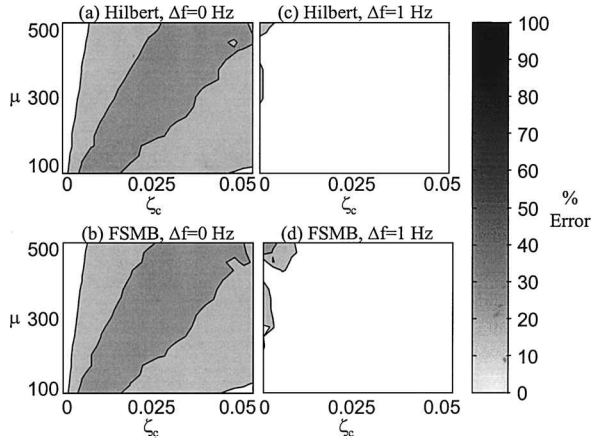

Fig. 10 Effects of a spectrally close mode with varied viscous damping ratio on the identified damping in a primary mode with varied coulomb damping ratio.

As a general rule, results will be best for modes that are separated by as large a frequency gap as possible. In this study, a separation of at least 1 Hz was desirable for best results. Good results were also obtained when there was no frequency separation between the two modes; however, care should be taken when analyzing data of this type to ensure that the envelope identified is truly indicative of the behavior of the mode of interest.

Effects of Close Mode Damping Level

To study the effect of the close mode damping level, an analytical signal was created that consisted of a primary mode of interest at 9 Hz and a close mode at 9 or 10 Hz. This results in a Δf of 0 or 1 Hz between the two modes. Note that the results for these close mode frequencies are symmetric about the primary mode frequency.[23] For example, a close mode of 8 Hz ($\Delta f = -1$ Hz) has essentially similar results to those of a close mode of 10 Hz ($\Delta f = +1$ Hz). The viscous damping ratio ζ of this close mode was varied from 0.00 to 0.05 in increments of 0.0025, and the resulting transients were analyzed using both the Hilbert analysis and the FSMB analysis. The percent error between actual and identified damping level was calculated, and contour plots of constant error are shown for coulomb damping in Fig. 10 and for quadratic damping in Fig. 11. It can be seen from Figs. 10a and 10b that, when the close mode has the same frequency as the primary mode of interest, both damping identification techniques have difficulty identifying the correct coulomb damping ratio. However, if the close mode is undamped, or if the coulomb damping ratio is small, the results improve slightly. If the close mode is shifted by as little as 1 Hz in either direction, the results improve significantly. In this case, for $\Delta f = 1$ Hz, the error is highest when the close mode is undamped and drops off rapidly when damping is added. This trend is also seen in the contour plots

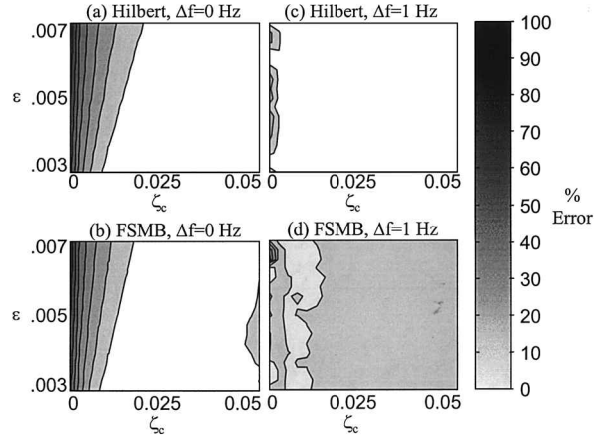

Fig. 11 Effects of a spectrally close mode with varied viscous damping ratio on the identified damping in a primary mode at 9 Hz with varied quadratic damping ratio.

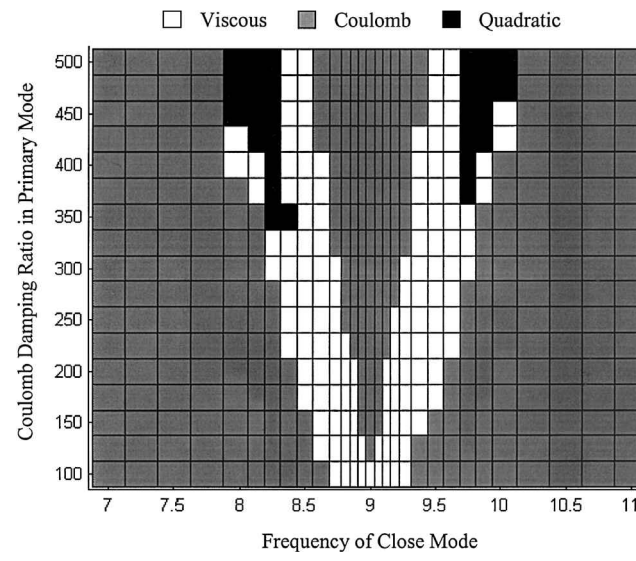

Fig. 12 Classifier results for a data set containing a primary mode with varied coulomb damping ratio and a close viscous mode with varied frequency.

of constant error for quadratic damping shown in Fig. 11 for both close mode Δf values (0 and 1 Hz).

Damping Mechanism Classification

A classification technique was developed to determine the dominant damping mechanism in a signal of unknown composition. The experimental envelope $\hat{a}(t)$ is first determined using either the Hilbert or the FSMB technique, and the analytical envelope expression for each damping mechanism under consideration is then fit to the experimental envelope. The rms error is then calculated for each fit as follows:

$$e_v = \sum_{t_k=t_1}^{t_n} \sqrt{a_v(t_k)^2 - \hat{a}(t_k)^2} \tag{19}$$

$$e_c = \sum_{t_k=t_1}^{t_n} \sqrt{a_c(t_k)^2 - \hat{a}(t_k)^2} \tag{20}$$

$$e_q = \sum_{t_k=t_1}^{t_n} \sqrt{a_q(t_k)^2 - \hat{a}(t_k)^2} \tag{21}$$

where $\hat{a}(t)$ is the envelope signal identified from the experimental data using the Hilbert damping analysis or the FSMB damping analysis and $a_v(t)$, $a_c(t)$, and $a_q(t)$ are the analytical expressions for the viscous, coulomb and quadratic envelope signals given in Table 1. The mechanism that results in the lowest rms error value

is determined to be the dominant damping mechanism in the data. Note that in many practical situations the identified dominant damping mechanism may not be the only damping mechanism present in the actual data. Figure 12 shows the classifier results for a matrix of analytically generated two mode data sets (the same set used to generate Fig. 8d), all with coulomb damping in the primary mode. In most instances, the classifier identifies the damping mechanism correctly, erring only in places where the error in identified damping level was high in Fig. 8d.

Conclusions

Damping identification in nonlinear systems can be complicated by many factors. Two damping identification techniques were considered, and the effects of data block length, noise, and error in assumed frequency on the accuracy of the identified damping parameters were assessed. Results and conclusions applicable to the nonlinear systems studied are listed as follows:

1) A moving block analysis was developed based on a Fourier series decomposition at the frequency of interest. This analysis performed well in identifying nonlinear damping levels in transients with coulomb and quadratic damping. This technique was relatively insensitive to noise in both the coulomb and quadratic damping cases. In addition, this method significantly reduced the computational load over the FFT-based moving block method, making it more amenable to online implementation.

2) The Hilbert transform-based damping analysis was shown to perform well for nonlinear damping mechanisms. In most cases it performs as well as or better than the Fourier series moving block analysis, and this technique is not a function of data block length. The Hilbert damping analysis has no frequency resolution difficulties, and is only slightly more sensitive to noise than the Fourier-series-based method. Finally, the Hilbert damping analysis is also much less computationally intensive when compared to the FFT-based moving block analysis, and so this technique may also be suitable for online implementation.

3) Both the Hilbert damping analysis and the Fourier-series-based damping analysis are relatively insensitive to small errors in the identified frequency of interest. As the frequency error increases, however, the error in the identified damping level will also increase, eventually to unacceptable levels. This problem can be avoided by using a standard steady-state frequency response function measurement with high-frequency resolution to identify the necessary parameters.

4) For spectrally close modes, if the close mode amplitude is high enough to significantly impact the transient, the error in the identified damping level will grow to unacceptable levels. It is, therefore, important to set the cutoff threshold used in the damping identification analysis to a level high enough to negate the impact of any persistent excitation from the close mode. Typically, a threshold set 10% or more above the level of the close mode will be sufficient. However, care must be taken not to set this threshold too high, or there will not be enough signal remaining to accurately identify the envelope geometry and damping ratio.

5) The spectral separation between the primary mode and a close mode can greatly affect the identified damping level. When the two modes have the same frequency, the results can be very good. However, if the modes are then separated by a small amount (<1 Hz), the error increases significantly. This problem is greatly mitigated if the modes are separated even further (≥ 1 Hz).

6) For a persistent excitation, the error in the identified damping level of a primary mode with quadratic damping can grow to unacceptable levels. This error is greatly reduced when even a small amount of damping is present in the close mode. This problem is not as severe in the coulomb damping case due to the simplified geometry of the coulomb envelope.

From these results, when used within their limits, the Hilbert-transform-based damping analysis and the Fourier-series-based damping analysis can be accurate and robust techniques for damping identification in nonlinear systems such as helicopter rotors.

Acknowledgments

This work was supported by the National Rotorcraft Technology Center under Grant NCC 2944, with Yung Yu serving as Technical Monitor.

References

[1]Hadjian, A. H., Masri, S. F., and Saud, A. F., "A Review of Methods of Equivalent Damping Estimation from Experimental Data," *Journal of Pressure Vessel Technology*, Vol. 109, May 1987, pp. 236–243.

[2]Kunz, D. L., "Influence of Elastomeric Damper Modeling on the Dynamic Response of Helicopter Rotors," *AIAA Journal*, Vol. 35, No. 2, 1997, pp. 349–354.

[3]Hausmann, G., and Gergely, P., "Approximate Methods for Thermo-viscoelastic Characterization and Analysis of Elastomeric Lead-Lag Dampers," *Proceedings of the Eighteenth European Rotorcraft Forum*, Association Aeronautique et Astronautique de France, Paris, 1992, pp. 88-1–88-17.

[4]Carlson, J. D., Catanzarite, D. M., and Clair, K. A. S., "Commercial Magneto-Rheological Fluid Devices," *International Journal of Modern Physics B*, Vol. 10, Nos. 23 and 24, 1996, pp. 2857–2865.

[5]Chopra, I., "Perspectives in Aeromechanical Stability of Helicopter Rotors," *Vertica*, Vol. 14, No. 4, 1990, pp. 457– 458.

[6]Smith, C. B., and Wereley, N. M., "Active–Passive Constrained Layer Damping of Composite Rotating Flexbeams," *Proceedings of the AIAA/ASME 37th Adaptive Structures Forum*, AIAA, Reston, VA, 1996, pp. 207–216.

[7]Smith, C. B., and Wereley, N. M., "Composite Rotorcraft Flexbeams with Viscoelastic Damping Layers for Aeromechanical Stability Augmentation," *M3D III: Mechanics and Mechanisms of Material Damping*, edited by A. Wolfenden and V. K. Kinra, ASTM STP 1304, American Society for Testing and Materials, West Conshohocken, PA, 1997, pp. 62–77.

[8]Kamath, G. M., Wereley, N. M., and Jolly, M. R., "Characterization of Magnetorheological Helicopter Lag Dampers," *Journal of the American Helicopter Society*, Vol. 44, No. 3, 1999, pp. 234–248.

[9]Yeager, W. T., Hamouda, M. H., and Mantany, W. R., "An Experimental Investigation of the Aeromechanical Stability of a Hingeless Rotor in Hover and Forward Flight," NASA TM 89107, AVSCOM TM 87-B-5, June 1987.

[10]McNulty, M. J., "Flap-Lag Stability Data for a Small-Scale Isolated Hingeless Rotor in Forward Flight," NASA TM 102189, AVSCOM TR 89-A-003, April 1989.

[11]Sharpe, D. L., "An Experimental Investigation of the Flap-Lag-Torsion Aeroelastic Stability of the Small-Scaled Hingeless Helicopter Rotor in Hover," NASA TP2546, AVSCOM TR 85-A-9, Jan. 1986.

[12]Tracy, A. L., and Chopra, I., "Aeroelastic Stability Investigation of a Composite Helicopter Rotors in Hover," *Journal of Aircraft*, Vol. 35, No. 5, 1998, pp 791–797.

[13]Tasker, F. A., "Damping Estimation in Helicopter Rotor Stability Testing," Ph.D. Dissertation, Dept. of Aerospace Engineering, Univ. of Maryland, College Park, MD, 1990.

[14]Hammond, C. E., and Doggett, J. R. V., "Determination of Subcritical Damping by Moving-Block/Randomdec Applications," *Proceedings of the NASA Symposium on Flutter Testing Techniques*, NASA CP-415, 1975, pp. 59–76.

[15]Bousman, W. G., and Winkler, D. J., "Application of the Moving-Block Analysis," *Proceedings of the AIAA 22nd Structures, Structural Dynamics, and Materials Conference*, AIAA, New York, 1981, pp. 755–763.

[16]Tasker, F. A., and Chopra, I., "Assessment of Transient Analysis Techniques for Rotor Stability Testing," *Journal of the American Helicopter Society*, Vol. 35, No. 1, 1990, pp. 39–50.

[17]Smith, C. B., and Wereley, N. M., "Transient Analysis for Damping Identification in Rotating Composite Beams with Integral Damping Layers," *Smart Materials and Structures*, Vol. 5, No. 5, 1996, pp. 540–550.

[18]Smith, C. B., and Wereley, N. M., "Nonlinear Damping Identification from Transient Data," *Proceedings of the 6th Annual International Symposium on Smart Structures and Materials*, SPIE—The International Society for Optical Engineering, Bellingham, WA, 1999.

[19]Bendat, J. S., and Piersol, A. G., *Random Data: Analysis and Measurement Procedures*, Wiley, New York, 1986, pp. 484–514.

[20]Agneni, A., and Crema, L. B., "Analytic Signals in the Damping Coefficient Estimation," *Proceedings of the International Conference on Spacecraft Structures and Mechanical Testing*, ESA, Noordwijk, The Netherlands, 1989, pp. 133–139.

[21]Simon, M., and Tomlinson, G. R., "Use of the Hilbert Transform in Modal Analysis of Linear and Non-Linear Structures," *Journal of Sound and Vibration*, Vol. 96, No. 4, 1984, pp. 421– 436.

[22]Smith, C. B., and Wereley, N. M., "Linear and Nonlinear Damping Identification in Helicopter Rotor Systems," *Proceedings of the AIAA 39th Structures, Structural Dynamics, and Materials Conference*, AIAA, Reston, VA, 1998, pp. 2473–2485.

[23]Smith, C. B., "Damping Identification in Helicopter Rotor Systems," Ph.D. Dissertation, Dept. of Aerospace Engineering, Univ. of Maryland, College Park, MD 1999.

A. Berman
Associate Editor